

# Foam Destruction by Mixed Solid–Liquid Antifoams in Solutions of Alkyl Glucoside: Electrostatic Interactions and Dynamic Effects

Krastanka G. Marinova and Nikolai D. Denkov\*

Laboratory of Chemical Physics Engineering,<sup>†</sup> Faculty of Chemistry, Sofia University,  
1 James Bourchier Avenue, 1164 Sofia, Bulgaria, and Rhodia Silicones,  
55 rue des Freres Perret, BP 22, 69191 Saint Fons Cedex, France

Received November 8, 2000. In Final Form: January 23, 2001

Antifoam substances are used in various technologies and commercial products to prevent the formation of undesirable foam. A typical problem in their application is that an antifoam that is rather active in a given surfactant solution might be very inefficient for other foaming media at comparable conditions. The reasons for this high antifoam selectivity to the used surfactant are still poorly understood. To gain a new insight into this problem, we compare the mechanisms of foam destruction by several antifoams for two surfactants: the nonionic alkyl- $C_{12/14}$ (glucopiranoside)<sub>1,2</sub> (APG) and the anionic sodium dioctyl-sulfosuccinate (AOT). Foam tests demonstrate significant differences in the antifoam activity for these two surfactants, although their entry, spreading, and bridging coefficients are very similar. One interesting feature is that the antifoams destroy APG-stabilized foams only under dynamic conditions (during shaking); the foam that “survives” the first several seconds after ceasing the agitation remains stable for many hours. In contrast, most of the studied antifoams destroy rapidly and completely the AOT-stabilized foams without external agitation. In general, the foams produced from APG solutions are significantly more stable. Additional model experiments show that the observed differences can be explained by three simple effects: (1) the kinetics of surfactant adsorption on the air–water and oil–water interfaces is much slower in APG solutions; (2) the barrier to entry of the antifoam globules is much higher for APG; (3) the films stabilized by APG are much thicker and more resistant to rupture by the antifoam globules. One surprising conclusion is that the electrostatic interaction between the charged air–water and oil–water interfaces is extremely important in solutions of the nonionic surfactant APG.

## 1. Introduction

Antifoams are used to prevent the formation of undesirable foam.<sup>1</sup> A typical antifoam consists of an oil (polydimethylsiloxane) or hydrocarbon, often pre-emulsified, dispersed hydrophobic solid particles, or a mixture of both.<sup>1–5</sup> The mixed solid–liquid antifoams are usually much more active than the individual components taken separately.<sup>2</sup> Several mechanisms of foam destruction by oil-containing antifoams were suggested in the literature,<sup>2–16</sup> and a comprehensive analytical review on this subject has been presented by Garrett.<sup>2</sup>

A variety of results<sup>2,5,17–19</sup> suggest that the stability of the asymmetric oil–water–air film, which forms when an antifoam globule approaches the surface of the foam film, is an important factor for the antifoam activity (Figure 1). If this asymmetric film is stable, the entry of the antifoam globules on the surface of the foam film is suppressed. As a result, the antifoam globules remain arrested in the aqueous phase without being able to destroy the foam. Following this idea, Garrett<sup>2</sup> suggested that the main role of the solid particles in mixed antifoams is to destabilize the asymmetric films, facilitating in this way the oil drop entry.

In parallel studies,<sup>20,21</sup> two related quantities were suggested to evaluate the stability of the asymmetric films: the energy of interaction per unit area,  $f$ , and the so-called “generalized entry coefficient”,  $E_g$ . The calculation of these quantities requires detailed information about the disjoining pressure,  $\Pi_{AS}(h)$ , which stabilizes the

\*To whom correspondence should be addressed: Dr. Nikolai D. Denkov, Laboratory of Chemical Physics Engineering, Faculty of Chemistry, Sofia University, 1 James Bourchier Ave., 1164 Sofia, Bulgaria. Phone: (+359) 2-962 5310. Fax: (+359) 2-962 5643. E-mail: ND@LTPH.BOL.BG.

<sup>†</sup> Formerly Laboratory of Thermodynamics and Physico-chemical Hydrodynamics.

(1) *Defoaming: Theory and Industrial Applications*; Garrett, P. R., Ed.; Marcel Dekker: New York, 1993; Chapters 2–8.

(2) Garrett, P. R. In *Defoaming: Theory and Industrial Applications*; Garrett, P. R., Ed.; Marcel Dekker: New York, 1993; Chapter 1.

(3) Pugh, R. J. *Adv. Colloid Interface Sci.* **1996**, *64*, 67.

(4) Aveyard, R.; Binks, B. P.; Fletcher, P. D. I.; Peck, T. G.; Rutherford, C. E. *Adv. Colloid Interface Sci.* **1994**, *48*, 93.

(5) Exerowa, D.; Kruglyakov, P. M. *Foams and Foam Films*; Elsevier: Amsterdam, 1998; Chapter 9.

(6) Ewers, W. E.; Sutherland, K. L. *Aust. J. Sci. Res.* **1952**, *5*, 697.

(7) Shearer, L. T.; Akers, W. W. *J. Phys. Chem.* **1958**, *62*, 1264, 1269.

(8) Prins, A. In *Food Emulsions and Foams*; Dickinson, E., Ed.; Royal Society of Chemistry Special Publication: London, 1986; Vol. 58, p 30.

(9) Bergeron, V.; Cooper, P.; Fischer, C.; Giermanska-Kahn, J.; Langevin, D.; Pouchelon, A. *Colloids Surf., A* **1997**, *122*, 103.

(10) Garrett, P. R.; Moor, P. R. *J. Colloid Interface Sci.* **1993**, *159*, 214.

(11) Garrett, P. R.; Davis, J.; Rendall, H. M. *Colloids Surf., A* **1994**, *85*, 159.

(12) Koczko, K.; Koczko, J. K.; Wasan, D. T. *J. Colloid Interface Sci.* **1994**, *166*, 225.

(13) Aveyard, R.; Cooper, P.; Fletcher, P. D. I.; Rutherford, C. E. *Langmuir* **1993**, *9*, 604.

(14) Robinson, J. V.; Woods, W. W. *J. Soc. Chem. Ind., London* **1948**, *67*, 361.

(15) Ross, S. *J. Phys. Colloid Chem.* **1950**, *54*, 429.

(16) Kulkarni, R. D.; Goddard, E. D.; Kanner, B. *Ind. Eng. Chem. Fundam.* **1977**, *16*, 472.

(17) Kruglyakov, P. M.; Taube, P. R. *Zh. Prikl. Khim.* **1971**, *44*, 129.

(18) Kruglyakov, P. M. In *Thin Liquid Films: Fundamentals and Applications*; Ivanov, I. B., Ed.; Surfactant Science Series, Vol. 29; Marcel Dekker: New York, 1988; Chapter 11.

(19) Kulkarni, R. D.; Goddard, E. D.; Kanner, B. *J. Colloid Interface Sci.* **1977**, *59*, 468.

(20) Lobo, L.; Wasan, D. T. *Langmuir* **1993**, *9*, 1668.

(21) Bergeron, V.; Fagan, M. E.; Radke, C. J. *Langmuir* **1993**, *9*, 1704.

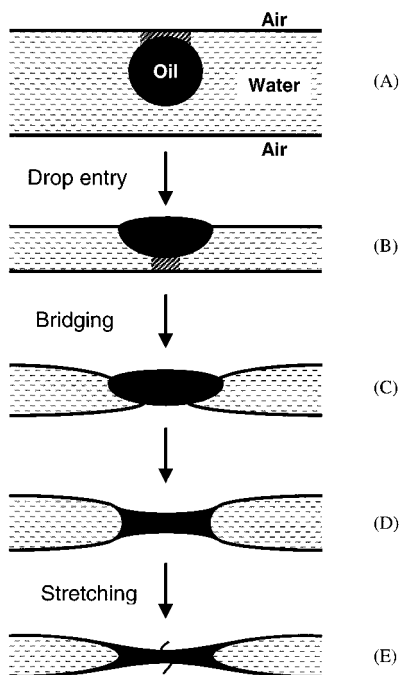


**Figure 1.** Bridging–stretching mechanism of foam film rupture (refs 25 and 27). The entry of the antifoam globule leads to the formation of an oil bridge (A–C), which is unstable; the bridge stretches with time, because of uncompensated capillary pressures at the oil–air and oil–water interfaces (C–E), and eventually ruptures in its center, destroying the entire foam film. The shaded areas in (A) and (B) show the asymmetric oil–water–air film.

asymmetric film. A difficulty for the practical application of this approach is that the disjoining pressure isotherm is rarely available, and hence a direct comparison of the values of  $f$  and  $E_g$  with the antifoam activity is still missing. First measurements, aimed to compare the stability of asymmetric oil–water–air films for some antifoam systems, were made by Koczo et al.<sup>12</sup> and Bergeron et al.<sup>9</sup> Their studies confirmed Garrett's hypothesis that the large asymmetric films are less stable if hydrophobic silica is present. Furthermore, Bergeron et al.<sup>21</sup> proved that the asymmetric films are indeed much less stable than the foam films.

A significant step forward in the quantification of the entry barrier was made by Hadjiiski et al.<sup>22</sup> These authors developed a new modification of the film trapping technique (FTT),<sup>23</sup> which allowed them to measure the critical capillary pressure,  $\Delta P_{CR}$ , leading to the entry of oil drops trapped in aqueous films (see section 2.2.5 for technical details). A higher value of  $\Delta P_{CR}$  corresponds to a higher barrier to drop entry and vice versa. An important advantage of the FTT is that it can be applied to micrometer-sized antifoam globules and viscous oils, which is often the case with commercial antifoams.

Another important issue concerns the structural element (foam film or Plateau border) that is actually destroyed by the antifoam globules. Most of the researchers consider that the *foam films* are ruptured by the antifoam, whereas Koczo et al.<sup>12</sup> suggest that the antifoam globules first escape from the foam films into the neighboring

Plateau borders (PB) and get trapped there; afterward, the globules destroy the PB and the neighboring foam films. Direct observations of foams and foam films by Basheva et al.<sup>24</sup> showed that the suggestion of Koczo et al.<sup>12</sup> was true when silicone oil (deprived of solid particles) was used as an antifoam. On the contrary, the foam destruction occurred through rupture of the foam films when mixed silica–silicone oil antifoam was used.<sup>25</sup> Therefore, both scenarios are possible depending on the particular system.

As discussed by Denkov et al.,<sup>24–26</sup> the structural element that is destroyed by the antifoam depends primarily on the entry barrier of the globules. If the barrier is low, the globules are able to enter the foam film surface and to rupture the film. However, if the barrier to drop entry is high, the drops could enter the air–water interface only after being strongly compressed by the walls of the narrowing Plateau borders, as a result of the water drainage from the foam. The time scale of the foam destruction process in these two cases is very different, on the order of seconds for very active (fast) antifoams, which destroy the foam lamellae, and on the order of minutes for slow antifoams destroying the PBs.<sup>24–26</sup>

Microscopic observations showed that the foam film destruction by typical antifoams, comprising a silicone oil and hydrophobic silica in solutions of the anionic surfactant sodium dioctyl-sulfosuccinate (AOT), occurs through the bridging–stretching mechanism<sup>25</sup> (Figure 1). This implies that unstable oil bridges are formed in the foam film, which stretch with time (because of uncompensated capillary pressures at the oil–air and oil–water interfaces<sup>27</sup>) and eventually rupture the film. The processes of antifoam exhaustion<sup>9,11,12,16,26</sup> and reactivation (by addition of a fresh portion of oil) were studied and explained for the same experimental system.<sup>26</sup> The knowledge accumulated for this particular system makes it a suitable reference point when other surfactants or antifoams are studied.

One important problem, deserving a systematic investigation, concerns the unexpectedly high selectivity of the antifoams and surfactants observed with many systems; antifoams that are very active in a given surfactant solution might be rather inefficient for another surfactant of similar properties (see, e.g., ref 24). This problem is well-known to practitioners and creates difficulties when a new surfactant formulation is introduced and a complementary antifoam has to be designed. To get some insight into this problem, we study the antifoam activity in solutions of the nonionic surfactant alkyl-polyglucoside (APG). As described below, the foam destruction occurs in a different manner in AOT and APG solutions. The reasons for this difference are analyzed from the viewpoint of the mechanism of antifoaming.

## 2. Experimental Details

**2.1. Materials. 2.1.1. Surfactants.** A commercial grade nonionic surfactant alkyl- $C_{12/14}$  (glucopiranoside)<sub>1,2</sub> of average molecular mass 495 Da is used in most experiments (commercial name Glucopon 600 CS UP, Henkel KGaA, Germany). For brevity, this surfactant is denoted as APG. Its concentration in the working solutions is 0.45 mM (unless another value is specified), which is 3 times the critical micellization concentration,  $cmc = 0.15$  mM. For comparison, some of the experiments are performed

(22) Hadjiiski, A.; Tcholakova, S.; Ivanov, I. B.; Gurkov, T. D.; Leonard, E. *Langmuir*, submitted. Hadjiiski, A.; Denkov, N. D.; Tcholakova, S.; Ivanov, I. B. *Proceedings of the 13th International Symposium on Surfactants in Solution (SIS-2000)*; Marcel Dekker: New York, 2001.

(23) Hadjiiski, A.; Dimova, R.; Denkov, N. D.; Ivanov, I. B.; Borwankar, R. *Langmuir* **1996**, *12*, 6665.

(24) Basheva, E.; Ganchev, D.; Denkov, N. D.; Kasuga, K.; Satoh, N.; Tsujii, K. *Langmuir* **2000**, *16*, 1000.

(25) Denkov, N. D.; Cooper, P.; Martin, J.-Y. *Langmuir* **1999**, *15*, 8514.

(26) Denkov, N. D.; Marinova, K. G.; Christova, C.; Hadjiiski, A.; Cooper, P. *Langmuir* **2000**, *16*, 2515.

(27) Denkov, N. D. *Langmuir* **1999**, *15*, 8530.

**Table 1. Composition of the Studied Antifoams**

antifoam	emulsion	contains silica	contains Span
silicone oil (PDMS)	no	no	no
compound A (CA)	no	yes	no
modified CA (MCA)	no	yes	yes
emulsion A (EA)	yes	yes	yes
analogue of EA (AEA)	yes	no	yes

in solutions of the anionic surfactant sodium dioctyl-sulfosuccinate,  $C_{20}H_{37}O_7SNa$ , Sigma catalog no. D-0885 (AOT), with a concentration of 10 mM (corresponding to 3.6 times the cmc = 2.8 mM).

**2.1.2. Antifoams.** Several antifoam formulations are studied (see Table 1):

(a) *Poly(dimethylsiloxane) Oil (PDMS)*. PDMS, of dynamic viscosity 1000 mPa s, is produced by Rhodia Silicones Europe (Saint Fons, France) under the commercial name 47V1000.

(b) *Compound A (CA)*. CA consists of PDMS oil and 4.2 wt % silica particles of pyrogenic origin (produced by flame hydrolysis of silicone tetrachloride; Degussa AG, Germany<sup>28</sup>). The silica makes large agglomerates in the compound, which have a fractal structure and a broad size distribution (from ca. 0.1 to 5  $\mu\text{m}$ ).

(c) *Emulsion A (EA)*. EA is a stable 10 wt % oil-in-water emulsion of compound A. It is further diluted to the desired final concentration in the surfactant solution. The stock emulsion is stabilized by two nonionic surfactants: sorbitan monostearate (Span 60) and ethoxylate of stearic acid with 40 ethoxy groups (stearyl-EO<sub>40</sub>, Mirj 52), both products of ICI Specialty Chemicals Ltd., U.K. Microscope observations show that this emulsion is polydisperse with drop diameters ranging from ca. 1 to 10 micrometers.

(d) *Other Formulations*. Our foam stability tests showed a strong effect of Span 60 (which is a solid substance, insoluble in water and PDMS at room temperature) on the antifoam activity; see section 3.1 below. For this reason, a mixture of compound A and Span 60 is prepared by introducing 5 wt % of Span under continuous stirring for 2 h at 70 °C (the mp of Span 60 is 57 °C). This sample contains both silica and Span 60 particles, and it is denoted hereafter as the "modified compound A" (MCA). Further, an emulsion of PDMS is prepared, following exactly the procedure for fabrication of emulsions A; the only difference is that this sample does not contain silica (denoted "analogue of emulsion A", AEA).

The antifoam concentration in the working surfactant solutions is 0.005 or 0.01 wt %, which is the typical range for mixed silica-silicone antifoams.

**2.2. Methods. 2.2.1. Foam Stability Evaluation (Shake Test).** A portion (100 mL) of the surfactant solution is poured in a 300 mL glass cylinder (4 cm in diameter). The antifoam is then added by using a micropipet M800 (Nichiryo Co., Tokyo, Japan), which is designed to supply small volumes (5–25  $\mu\text{L}$ ) of viscous compounds. The cylinder is tightly plugged by a bung, and the foam is generated by 30 vigorous up-and-down hand shakes. The initial volume and the kinetics of destruction of the obtained foam are monitored for 2 min. Then, another shaking cycle is performed by 30 new up-and-down shakes of the cylinder. In this way, the change of the foam volume with the number of the shaking cycle (viz., the antifoam exhaustion) is monitored.

A small amount (2–3 mL) of the surfactant solution is taken after some of the shaking cycles for light scattering determination of the antifoam globule size. Because the volume of the surfactant solution noticeably decreases after taking several samples, in the figures below we show the foam volume divided by the solution volume (i.e., the relative foam volume).

**2.2.2. Dynamic Light Scattering (DLS).** The variation of the globule size with the antifoam exhaustion (see section 2.2.1) is studied by DLS. The system 4700C (Malvern Instruments, Malvern, U.K.), equipped with an argon laser operating at 488 nm light wavelength and with a 7032 CE 8-bit correlator, is used. This setup measures the diffusion coefficient of the dispersed antifoam globules. The size distribution of the globules is afterward calculated by using the Stokes-Einstein relation

$$d = \frac{kT}{3\pi\eta D} \quad (1)$$

and the Multimodal software of Malvern;  $d$  is the hydrodynamic particle diameter,  $kT$  is the thermal energy,  $\eta$  is the dynamic viscosity of the disperse medium, and  $D$  is the diffusion coefficient. The method is applicable to particles of size varying between ca. 5 nm and 5  $\mu\text{m}$ . Because the antifoam globules exhibit a broad size distribution, the calculated mean size for a given sample depends on the employed procedure of averaging. The volume average diameter,  $\langle d_v \rangle$ , is quoted below, because this value is determined relatively reliably by DLS and because it represents the typical size of the globules containing most of the dispersed PDMS oil.

**2.2.3. Optical Observation of Foam Films.** Two types of foam films are formed and observed: horizontal films of millimeter size and vertical films suspended on a rectangular frame of centimeter size. Millimeter sized foam films are observed in reflected monochromatic light by using the method of Scheludko and Exerowa.<sup>29,30</sup> The film is formed from a biconcave drop placed in a short capillary (i.d. 2.5 mm, height 4 mm) by sucking out liquid through a side orifice. Fiber optic illumination of the film and a long-focus lens (CTL-6, Tokyo Electronic Industry Co., Ltd.) attached to a charge-coupled device (CCD) camera (Panasonic WV-CD20) are used. The interference of the light reflected from the two surfaces of the foam film leads to the appearance of dark and bright interference fringes, corresponding to a given film thickness. The difference,  $\Delta h$ , in the film thickness between two neighboring dark (or two neighboring bright) fringes is equal to<sup>31,32</sup>

$$\Delta h = \lambda/2n \approx 203 \text{ nm} \quad (2)$$

where  $\lambda \approx 540 \text{ nm}$  is the wavelength of the illuminating light and  $n = 1.33$  is the refractive index of the solution.

Vertical films are formed on a rectangular glass frame (2 × 3 cm, made from 3 mm glass rod), which is attached to a specially designed sliding mechanism.<sup>25</sup> The latter is driven by a powerful spring, which ensures a rapid withdrawal of the frame from the surfactant solution for 40–50 ms. The experiment is made in a closed glass container (to reduce the water evaporation from the films) with optically clean walls. These films are observed in reflected white light (stroboscope ST250-RE, PHYLEC) by means of a long-focus zoom lens (LMZ 45C5, Japan Lens Inc.) attached to a high-speed camera (HSV-1000, NAC Europe, 1000 frames per second).

A major advantage of these methods is that experiments can be performed with real antifoams, dispersed as micrometer sized globules, just as in the case for practical systems.

**2.2.4. Observation of Asymmetric Oil-Water-Air Films.** An asymmetric film of millimeter size is formed by pressing a drop of oil or compound (which is blown out from a capillary of 1.2 mm i.d.) against the solution surface from below; see Figure 2. The capillary is mounted on an XYZ-stage, which allows one to adjust the drop position. A syringe driven by a micrometer screw is connected to the capillary and is used to control the drop radius. These films are observed from above in reflected light using the optical system described in section 2.2.3 for small foam films. The experimental cell is covered by an optically clean glass window to suppress the water evaporation from the film.

**2.2.5. Film Trapping Technique (FTT).** A schematic presentation of the principle of FTT<sup>22,23</sup> is shown in Figure 3. A vertical capillary, partially filled with the working solution, is placed in a close vicinity above the glass substrate. The capillary is connected to a pressure control system, which allows one to vary and to measure the difference,  $\Delta P = (P_{\text{IN}} - P_0)$ , between the air pressure in the capillary,  $P_{\text{IN}}$ , and the ambient atmospheric pressure,  $P_0$ . When  $P_{\text{IN}}$  is increased, the air-water meniscus in the capillary is pushed against the glass, and a wetting film is formed, which traps some of the oil drops (antifoam globules)

(29) Scheludko, A.; Exerowa, D. *Kolloid-Z.* **1957**, *155*, 39.

(30) Scheludko, A. *Adv. Colloid Interface Sci.* **1967**, *1*, 391.

(31) Vasicek, A. *Optics of Thin Films*; North-Holland: Amsterdam, 1960.

(32) Born, M.; Wolf, E. *Principles of Optics*, 6th ed.; Pergamon: Oxford, 1980.

(28) Degussa Technical Bulletin No 42 (*Synthetic Silicas for Defoamers*), 3rd ed.; Degussa AG: Frankfurt, Germany, 1988.

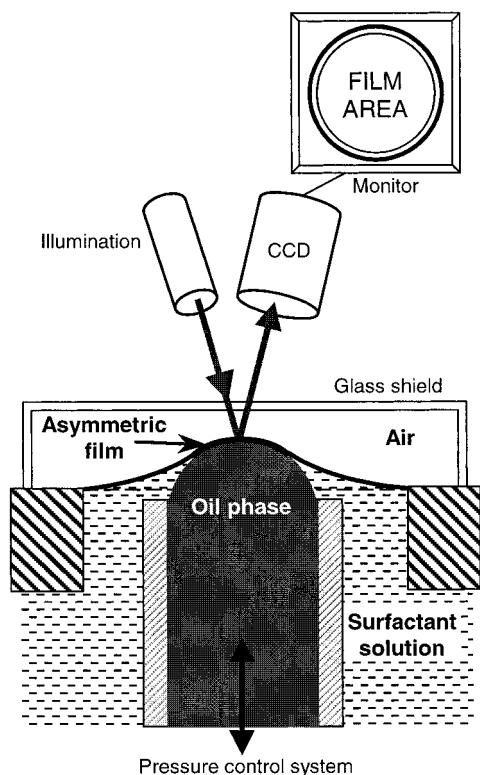


**Figure 2.** Schematic presentation of the setup for observation of asymmetric oil-water-air films by pressing a drop of oil (or compound) underneath the solution surface. The films are observed from above in reflected monochromatic light. An optically clean glass cover is used to suppress the water evaporation.

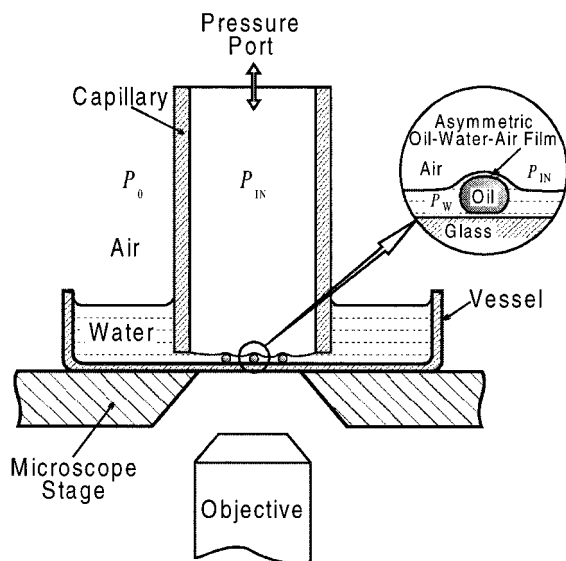


**Figure 3.** Scheme of the experimental setup used in the film trapping technique for measuring the critical capillary pressure, which leads to entry of the antifoam globules (ref 22).

dispersed in the working solution. These drops remain sandwiched between the air-water and glass-water interfaces. The droplets are observed from below, through the glass substrate, by means of an inverted optical microscope. Upon further increase of the capillary pressure,  $\Delta P$ , the trapped drops enter the air-water interface. Thus, the critical capillary pressure inducing a drop entry,  $\Delta P_{CR}$ , is measured as a function of the solution composition and drop radius.

**2.2.6. Surface Tension Measurements and Oil Spreading Experiments.** The equilibrium surface tension of the aqueous solutions is measured by the Wilhelmy plate method (Kruss K12

**Table 2. Volume of the Foam Generated by 30 Up-and-Down Shakes in a Glass Cylinder Containing 0.45 mM APG Solution and 0.005 wt % of Antifoam**

antifoam	initial foam volume $V_{IN}$ , mL	foam volume 2 min after shaking, mL
no antifoam	120–130	120–130
PDMS	110–120	110–120
CA	100–110	100–110
MCA	30–40	10–20
EA	30	10
AEA	30–40	30–40

tensiometer). The platinum plate is cleaned before each measurement by immersion in hydrofluoric acid and heating in a flame. The dynamic surface tension,  $\sigma(t)$ , is measured by the maximum bubble pressure method (MBPM). The experimental setup described in ref 33 is employed without the detailed analysis of the bubble expansion process used there.

The rate of oil spreading was evaluated by using the procedure from refs 9 and 26. A glass petri dish of diameter 20 cm and depth 2 cm is filled with surfactant solution, and trace particles (hydrophobized silica) are sprinkled over the solution surface. A thin glass rod, whose tip has been soaked by silicone oil, is gently placed in contact with the solution surface by using a micrometer drive device. The radial motion of the trace particles, indicating the front of the spreading oil, is recorded by a CCD camera. The video records are afterward processed, and the period needed for the oil to spread up to 5 cm radial distance from the oil source is measured. At least four independent experiments are performed with each sample. All experiments are carried out at the ambient temperature ( $23 \pm 1$  °C).

### 3. Experimental Results and Discussion

First, the main results from the foam tests with APG solutions are presented and compared to the results obtained with AOT solutions. The model experiments are described afterward and used to explain the observed differences in the antifoam activity.

**3.1. Foam Tests. 3.1.1. Comparison of the Antifoam Activity.** In Table 2, we compare the volumes of the foams, produced from 0.45 mM APG solutions in the presence of 0.005% PDMS, CA, MCA, EA, or AEA. Data for the initially generated foam,  $V_{IN}$ , and for the foam left after 2 min are shown. The top of the foam was relatively flat, which allowed us to measure the foam volume with an accuracy better than  $\pm 5$  mL. The foam destruction process was regular, with the bubble coalescence taking place mainly in the top layer.

The experiments demonstrate that  $V_{IN}$  strongly depends on the applied antifoam, but in most systems (except MCA and EA) the foam volume remains constant after the shaking has been stopped. In the systems containing MCA and EA, there is some foam destruction during the first several seconds of the quiescent period (from 30–40 down to 10–20 mL) but afterward the foam remains stable for many hours. In other words, the antifoams are active only under dynamic conditions (during mechanical agitation) in APG solutions. Moreover, the addition of concentrated EA on the top of a preformed, static foam column does not lead to destruction; the antifoam globules are seen to enter the PBs without inducing a foam rupture. In contrast, CA and EA are able to destroy entirely the foams produced from 10 mM AOT solutions within seconds, without any external agitation.<sup>25,26</sup> In general, the studied antifoams are much more active in AOT than in APG solutions.

Let us compare the activity of the different antifoams in APG solutions. The data in Table 2 show that PDMS and CA have a little influence on  $V_{IN}$ . Most active is EA,

(33) Horozov, T. S.; Dushkin, C. D.; Danov, K. D.; Arnaudov, L. A.; Velez, O. D.; Mehreteab, A.; Broze, G. *Colloids Surf., A* **1996**, *113*, 117.

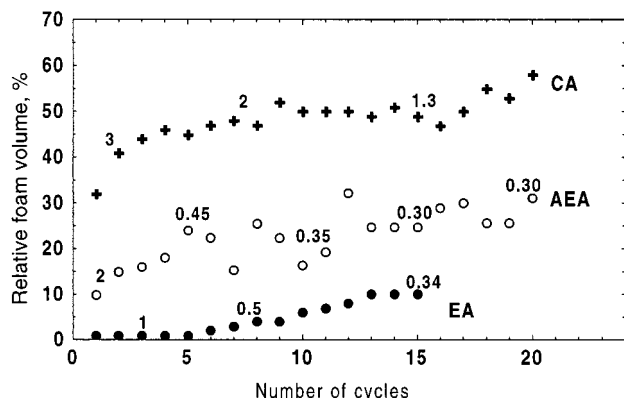


**Figure 4.** Foam volume as a function of the number of the foam production/destruction cycle for 0.45 mM APG solutions containing 0.01% EA, AEA, or CA. The foam volume is measured 1 min after the shaking cycle has been stopped. The numbers on the curves designate the particle diameters (in micrometers) as measured by DLS.

whereas AEA and MCA are slightly worse than EA but are much better than PDMS and CA. Note that although CA and EA contain the same oil and silica particles, their antifoam efficiencies are very different. On the other hand, the two active emulsions, EA and AEA, contain Span (in the form of solid particles) and Mirj and differ only in the absence of silica in AEA; see Table 1. All these results, along with the fact that MCA (which contains Span and does not contain Mirj) is much more active than CA, show that the key component separating the active from inactive compounds is Span. One can conclude that the high activity of EA, AEA, and MCA is due mainly to the presence of Span, and the silica in EA, MCA, and CA has a smaller effect on their activity in APG solutions. Although the silica is less important as an antifoam component than Span for APG solutions, one sees from Table 2 that the most active are EA and MCA, which contain both silica and Span particles (i.e., a synergistic effect is observed). In sharp contrast, it was proven<sup>26</sup> for AOT solutions that the silica is very important for the antifoam activity, whereas Span and Mirj have a minor effect.

### 3.1.2. Antifoam Exhaustion and Reactivation.

Figure 4 presents the exhaustion curves (foam volume versus number of shaking cycle) in APG solutions containing 0.01% of different antifoams. As discussed in ref 26 (see Figure 11 therein), the antifoam exhaustion in AOT solutions is due to (1) segregation of the silica and silicone oil into two inactive populations of antifoam globules, silica-free and silica-enriched, and (2) disappearance of the spread oil layer from the solution surface. No significant reduction of the antifoam globule size was observed during exhaustion in AOT. The antifoam can be reactivated by addition of fresh PDMS.<sup>26</sup> The reactivation was explained by a recombination of the silica-enriched globules with the newly added oil, which resulted in the formation of antifoam globules of an optimal silica/oil ratio.

The change of the average globule size upon exhaustion of CA, EA, and AEA in APG solutions was monitored by DLS; see the numbers associated with the curves in Figure 4. A clear tendency of decrease of the globule size is observed in each of these systems. However, the comparison of the results for the various antifoams shows that the larger globule size does not necessarily mean a higher activity; for example, the globules in CA are larger than those in EA, but CA is substantially less active.

Figure 5 presents the series of (i) exhaustion of 0.005% EA, (ii) reactivation by 5  $\mu$ L of PDMS, (iii) a second exhaustion, (iv) a second reactivation, and (v) another

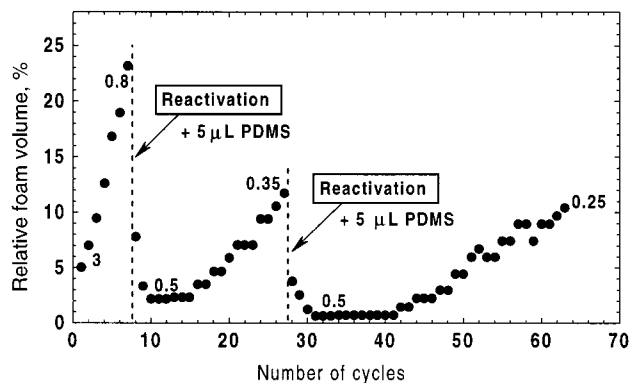


**Figure 5.** Consecutive series of exhaustion and reactivation of EA (foam volume versus cycle number). First, 0.005 wt % EA is exhausted in 100 mL of 0.45 mM APG solution (cycles 1–7). Afterward, 5  $\mu$ L PDMS is added to this sample; antifoam reactivation is observed, followed by another exhaustion (cycles 8–27). A subsequent reactivation–exhaustion series is made in cycles 28–64.

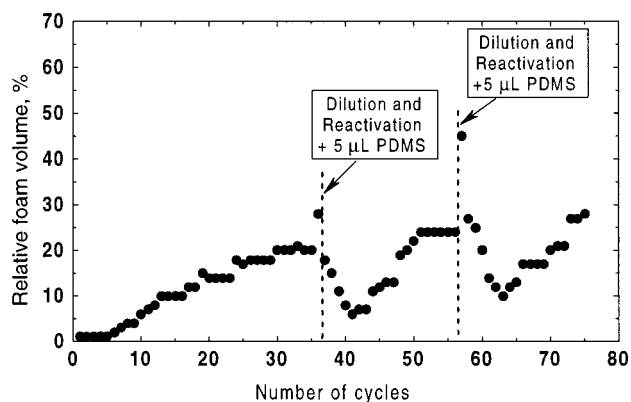


**Figure 6.** Reactivation with dilution (foam volume versus cycle number). The foaming solution, 0.45 mM APG, initially contains 0.01 wt % (10  $\mu$ L) of EA. After its exhaustion, the sample is diluted twice with pure surfactant solution and 5  $\mu$ L of PDMS is added (36th cycle). A reactivation of the antifoam is observed, followed by another exhaustion (cycles 37–56), and so forth.

exhaustion. The average globule diameter is also shown. The globule size immediately after the sample reactivation is not significantly larger than that in the exhausted samples and is certainly much smaller than the average globule size in the initial active EA. Therefore, one cannot attribute the reactivation to an increase of the average size of the antifoam globules. In general, there is no correlation between the measured size of the globules and the antifoam activity in these experiments. Instead, it was possible to correlate the exhaustion with the disappearance of the spread oil layer on the solution surface (see section 3.7). Similar conclusions were previously drawn from the foam tests with AOT solutions,<sup>26</sup> which allows us to speculate that the mechanisms of exhaustion and reactivation are similar with both surfactants.

To check whether the reactivation was not a trivial effect of the increased total concentration of oil, we modified the experimental procedure. After 0.01% (10  $\mu$ L) of EA was exhausted in APG solution, the latter was diluted twice by surfactant solution (without antifoam) and then 5  $\mu$ L silicone oil was added; see Figure 6. Thus, the total antifoam concentration remained the same, 0.01 wt %. A noticeable reactivation was observed again (though not so significant as in the absence of dilution), which proved that the reactivation was not a simple concentration effect. Note the gradual improvement of the antifoam activity

during the first several cycles after each reactivation in Figures 5 and 6; this improvement reflects the ongoing process of silica–oil recombination and the formation of more active antifoam globules.

Foam tests with APG solutions containing 10 mM NaCl showed that the electrolytes reduce significantly the rate of exhaustion of EA (0.01 wt %). As explained below, the electrolytes affect the antifoam activity in APG solutions, because the thickness and the stability of the foam and asymmetric films depends on the electrostatic repulsion between their surfaces.

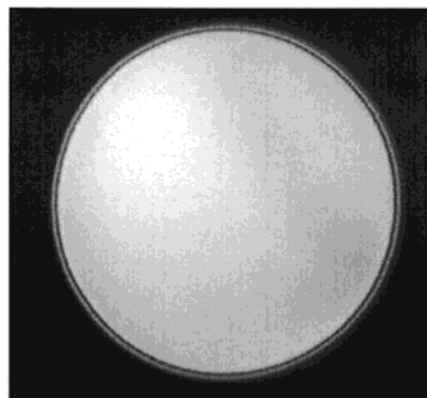
**3.2. Stability of Foam Films. 3.2.1. Small Films in the Capillary Cell.** A remarkable feature of the films made from APG solution in the absence of antifoam is that their equilibrium thickness is very large (100–130 nm). For comparison, the equilibrium thickness of AOT-stabilized films is an order of magnitude smaller (10–15 nm). Otherwise, the dynamics of film thinning is similar for these two surfactants (see refs 25 and 26 for details). The relatively large equilibrium thickness of the APG-stabilized films can be explained by the low concentration of ions in the solution (low ionic strength) and by the fact that the air–water interface possesses a negative surface charge in the presence of nonionic surfactants.<sup>34–37</sup> As a result, there is a long-range electrostatic repulsion between the surfaces of the foam film. The role of the electrostatic forces can be easily demonstrated by making films from APG solution containing an electrolyte. The equilibrium film thickness is  $\sim 10$  nm for solutions containing 10 mM NaCl; see Figure 7.

Note that even in the absence of any external salt, the ionic strength in 10 mM AOT solutions is high owing to the surfactant dissociation. The ion concentration in a micellar solution can be estimated to be<sup>38</sup>

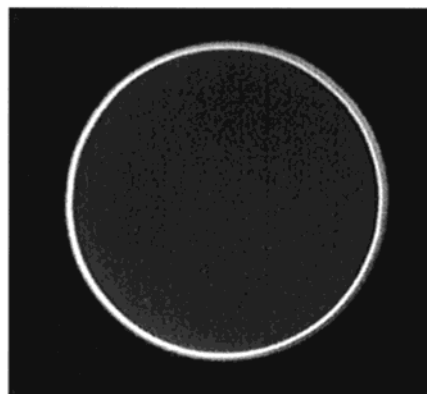
$$C_{\text{ION}} = 2 \text{ cmc} + \alpha(C_{\text{S}} - \text{cmc}) \quad (3)$$

where  $C_{\text{S}}$  is the total surfactant concentration,  $\alpha$  is the degree of dissociation of the surfactant molecules in the micelles, and the free monomers are considered as completely dissociated. Assuming  $\text{cmc} = 2.8$  mM and  $\alpha \approx 0.2$ , one can estimate that  $C_{\text{ION}}$  in 10 mM AOT solution is about 7 mM; that is, the Debye screening length  $\kappa^{-1} \approx 5$  nm. On the other hand, ions in APG solutions are generated only by dissociation of carbonic acid, which is formed as a result of  $\text{CO}_2$  dissolution from the atmosphere. The ionic strength of such solutions is on the order of  $10^{-5}$  M, which corresponds to  $\kappa^{-1} \approx 100$  nm. Thus, one can explain the different thicknesses of the equilibrium foam films by the ionic strengths of the APG and AOT solutions.

Then, we studied foam films from 0.45 mM APG solutions containing 0.01 wt % of EA. Foam tests with this solution showed that EA was a very efficient antifoam (see Figures 4 and 6). Nevertheless, the foam films formed in the capillary cell from the same solution were very stable; no film rupture was observed at all. Many antifoam globules were initially trapped in the foam films; however, all these globules left the film during its thinning without changing the film thinning pattern and the equilibrium thickness. For comparison, the foam films formed from AOT solutions containing 0.01% EA were very unstable



(A)



(B)

**Figure 7.** Equilibrium foam films of diameter 1 mm, obtained from 0.45 mM APG solution in the capillary cell (refs 29 and 30). (A) No electrolyte is added, and the film has an equilibrium thickness of 120 nm, because of a long-range electrostatic repulsion. (B) The solution contains 0.01 M NaCl, and the equilibrium thickness is only 15 nm, because the electrostatic repulsion is screened.

in the capillary cell and ruptured within seconds at a relatively large thickness.<sup>25,26</sup>

Let us note that the foam film surfaces in the capillary cell are saturated with adsorbed molecules (typically, the film is made several minutes after the moment of placement of the surfactant solution into the experimental cell, that is, after the air–water surfaces are formed). Therefore, the films in the capillary cell resemble the films in a still foam, where the surfactant adsorption layers are complete. In contrast, during foaming, fresh air–water interfaces are continuously formed, which are not covered by dense adsorption layers. The fact that the foam destruction in APG solutions occurs mainly during foaming (see section 3.1.1 and Table 2) evidences that the studied antifoams are active only in APG-stabilized films, whose adsorption layers are still incomplete. Once the equilibrium adsorption layers are formed (similar to those in the capillary cell), the antifoam globules are unable to enter the surfaces of the foam films and the latter remain stable.

To mimic to some extent the stability of foam films having incomplete adsorption layers, we made experiments with APG solutions of concentrations below the cmc. The foam films from 0.01 mM APG were stable in the absence of antifoam, and the final film thickness was about 180 nm. This larger equilibrium thickness at a lower surfactant concentration is not surprising, because it has been shown by several authors<sup>34,35,39</sup> that the bare oil–water and air–water interfaces possess a significant

(34) Exerowa, D.; Zacharieva, M. In *Research in Surface Forces*; Consultants Bureau: New York, 1975; Vol. 4.

(35) Waltermo, A.; Claesson, P. M.; Simonsson, S.; Manev, E.; Johansson, I.; Bergeron, V. *Langmuir* **1996**, *12*, 5271.

(36) Pugh, R. G.; Yoon, R.-H. *J. Colloid Interface Sci.* **1994**, *163*, 169.

(37) Bergeron, V.; Waltermo, A.; Claesson, P. M. *Langmuir* **1996**, *12*, 1336.

(38) Richetti, P.; Kekicheff, P. *Phys. Rev. Lett.* **1992**, *68*, 1951.

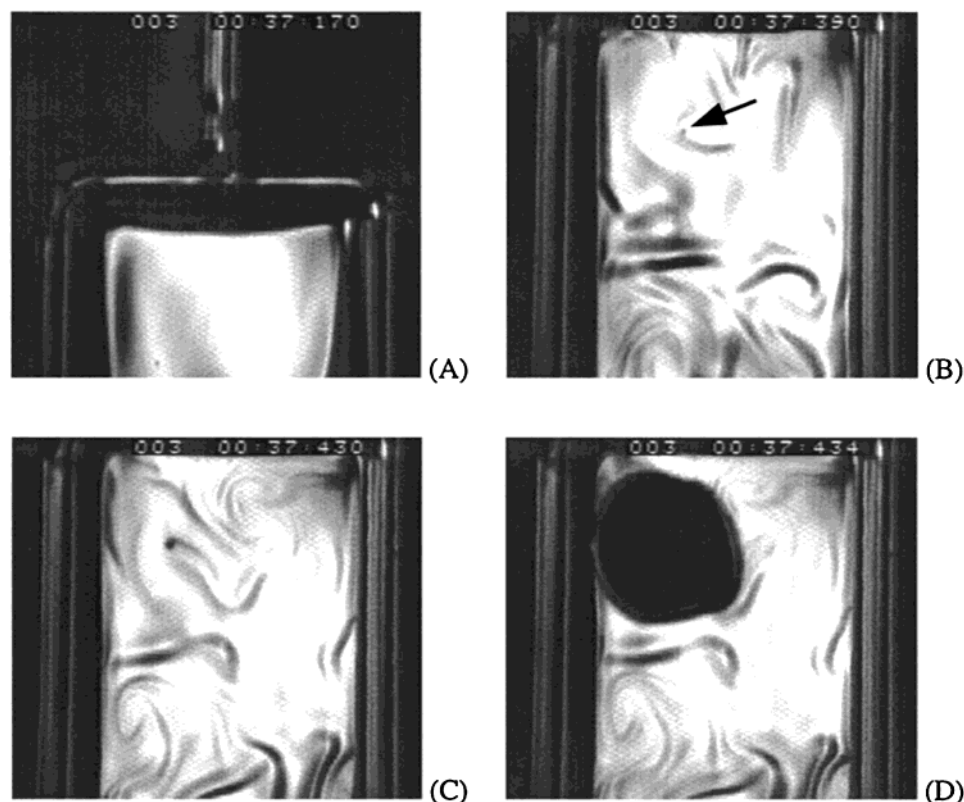


**Figure 8.** (A) Vertical foam film formed by withdrawal of a rectangular glass frame from 0.45 mM APG solution containing 0.01% EA. (B) An antifoam globule enters and bridges the two film surfaces about 0.2 s after film formation. The oil bridge stretches with time until (D) a hole is formed and the foam film ruptures. The film is observed in reflected white light by a high-speed video camera (note the timer in the upper part of the pictures).

negative electrical charge at neutral pH. The adsorption of nonionic surfactants on these interfaces decreases the magnitude of this potential.<sup>34–36,39,40</sup> Thus, the thicker films at lower surfactant concentrations can be explained by the increased surface potential at virtually unchanged ionic strength. The addition of 0.01% of EA in this solution resulted in very unstable foam films in the capillary cell. These films ruptured at a large thickness, within a few seconds after their formation, as in the experiments with 10 mM AOT. The antifoam globules entered the film surfaces, and the characteristic interference pattern called “the fish eye”<sup>25</sup> was frequently observed just before film rupture. As explained in refs 25 and 26, the fish eye indicated the formation and stretching of an oil bridge, which showed that the antifoam destroyed APG films by the same mechanism, which was found with AOT solutions (Figure 1).

**3.2.2. Large Vertical Films.** The films formed from 0.45 mM APG solution without antifoam were stable, whereas those formed in the presence of 0.01% of EA or AEA ruptured almost immediately, within 0.1–0.3 s after their formation, at large thicknesses (above several  $\mu\text{m}$ ). The process of film rupture in the presence of EA was observed with a high-speed video camera. As in the experiments with AOT,<sup>25</sup> in most cases we were able to locate the position of film rupture; see Figure 8. In some of the runs, the films were ruptured by large oil lenses floating on the foam film surface and containing big silica particles, whereas in other experiments the rupture was caused by antifoam globules entering from the film interior.

The low stability of the vertical foam films (cf. with the stable films in the capillary cell) can be explained by two effects: (1) the rate of surface expansion during formation of the vertical films is very high, so the film surfaces are

not saturated with adsorbed surfactant; (2) the area of the vertical films is almost 3 orders of magnitude larger as compared to the area of the films in the capillary cell, and hence it is more probable to capture very active, “lethal” antifoam globules in the vertical film. The foam tests imply that both effects are important: The fact that the foam is destroyed only under dynamic conditions demonstrates the importance of effect 1. On the other hand, the size of the foam bubbles formed in the presence of antifoam is substantially smaller than the bubble size in the absence of antifoam, which indicates that the larger foam films are destroyed with higher probability, effect 2.

**3.3. Asymmetric Oil–Water–Air Films.** The aim of these experiments was to get some insight into the factors affecting the entry of the antifoam globules in APG and AOT solutions.

A picture of the asymmetric film, formed when a drop of compound A is pressed against the surface of 0.45 mM APG solution, is shown in Figure 9A. The films are rather thick (because of the electrostatic repulsion between their surfaces) and do not rupture even at the highest accessible capillary pressure, 100 Pa. No solid particles are seen to protrude across the film, and its appearance is similar to that in experiments with pure PDMS. Therefore, one may speculate that the relatively high stability of the asymmetric films and the low activity of CA in APG solutions are due to (1) the large thickness of the asymmetric film and (2) the small penetration depth of the solid particles into the aqueous phase (Figure 10).

(39) Marinova, K. G.; Alargova, R. G.; Denkov, N. D.; Veleev, O. D.; Petsev, D. N.; Ivanov, I. B.; Borwankar, R. P. *Langmuir* **1996**, *12*, 2045.

(40) Ivanov, I. B.; Marinova, K. G.; Alargova, R. G.; Denkov, N. D.; Borwankar, R. P. *Proceedings of Second World Congress on Emulsion*; EDS: Bordeaux, 1997; Vol. 2, 2-2-149.

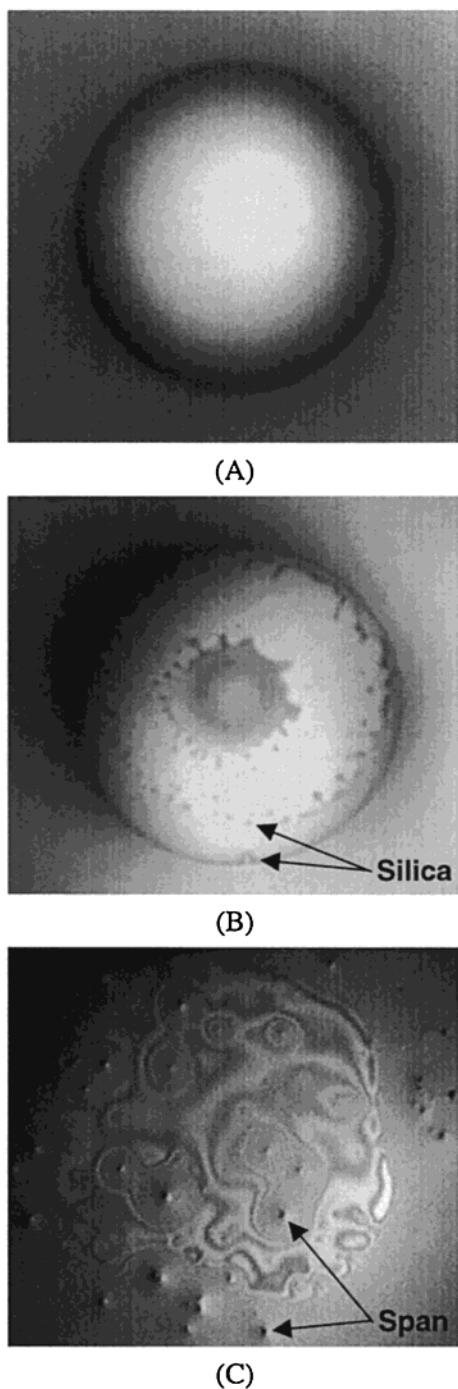


**Figure 9.** Asymmetric oil–water–air films as observed in the setup from Figure 2: (A) compound A in 0.45 mM APG, (B) compound A in 10 mM AOT, and (C) modified compound A in 0.45 mM APG. Note the uniform thickness of the film in (A); no particles are seen to protrude and the film is very stable, whereas many particles are seen to protrude in (B) and (C) and the films are unstable.

In contrast, the asymmetric films formed with CA in 10 mM AOT solutions have a thickness  $<20$  nm and many solid particles are seen to protrude across the films (Figure 9B). Not surprisingly, these films are very unstable and easily rupture. In several experiments, we were able to monitor the process of rupture and to locate the protruding silica particle that caused it.

We carried out similar experiments with MCA in APG solutions. Many big Span particles were seen in the asymmetric films (Figure 9C). Most of these films rup-

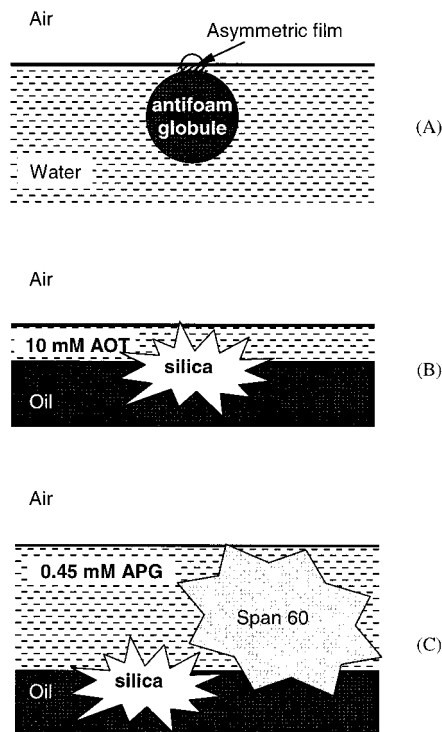


**Figure 10.** Schematic presentation of the film thickness and of the positions of silica and Span particles in the asymmetric oil–water–air films, formed (A) when an antifoam globule approaches the foam film surface: (B) in AOT solutions and (C) in APG solutions.

tured, and frequently we were able to detect the Span particle that caused the film bursting.

The above observations correlate well with the results from the foam tests (Table 1). Furthermore, they demonstrate the important role of the solid Span particles not only for the stabilization of the antifoam emulsions (which is the primary reason to use Span in commercial formulations) but for the foam destruction process in APG solutions as well. As mentioned above, Span has no significant effect on the antifoam activity in AOT solutions.<sup>26</sup>

**3.4. Barriers to Drop Entry.** These experiments are performed with antifoam globules of diameters ranging between 1 and  $10\ \mu\text{m}$ . The obtained data are very scattered. That is why the results are presented in Table 3 as ranges of capillary pressure, in which globule entry events are observed, along with an estimate of the fraction of globules that enter in the respective range.

The critical capillary pressure for PDMS drops is above 1250 Pa (the upper limit of our setup). This capillary pressure corresponds to the hydrostatic pressure at the top of a 12 cm foam column. Therefore, the entry of PDMS drops in short static foams is improbable, and this explains why PDMS is inactive in APG solutions; cf. Table 2 (for discussion of the connection between the critical capillary pressure measured by FTT and the hydrostatic pressure in the foam column, see section 4.1 in ref 24). The entry barrier for the same oil in AOT solutions<sup>22</sup> is only 30 Pa, which corresponds to the hydrostatic pressure at the top of a 0.3 cm foam column. This explains why PDMS has some activity in AOT solutions by the mechanism discussed in ref 24; the initially produced voluminous foam is slowly destroyed by oil drops, captured in the Plateau borders (within 15 min, the foam volume decreases from 150 to 15 mL).

**Table 3. Critical Capillary Pressure,  $P_c^{CR}$  [Pa], Leading to Globule Entry for Different Antifoams in APG Solutions, As Determined by FTT (See Section 3.4)**

APG concentration	antifoam			
	47V1000	compound A	emulsion A	modified CA
0.45 mM, $3 \times \text{CMC}$	>1250	120–1250 (5%) >1250 (95%)	120–1250 (50%) >1250 (50%) (in 10 mM NaCl 5–200 Pa, 95%)	120–1250 (70%) >1250 (30%)
0.045 mM, $0.33 \times \text{CMC}$		<10 (95%)	<10 (95%)	

FTT experiments with CA in APG solutions show that most of the observed droplets ( $\sim 95\%$ ) do not enter the air–water interface even at the highest accessible pressure (1250 Pa). Only some of the globules (about 5%) enter at lower pressures, scattered in the range from 120 to 1250 Pa. Most of these globules contain big silica particles, which are visible in the optical microscope. Probably, only such big particles are able to pierce the relatively thick APG films and to induce a drop entry (Figure 10). As expected, the entry barriers for the globules of EA and MCA (both containing Span particles) are lower; more than 50% of the globules enter in the range between 120 and 1250 Pa. Still, these barriers are much higher than those measured for EA and CA in AOT solutions (below 15 Pa). The fact that the entry barriers for all antifoams in APG solutions are rather high (above 120 Pa) explains why the APG-stabilized foams are stable under static conditions. As discussed in refs 24–27, the entry barrier should be below a certain critical value (20 Pa) to have a fast antifoam that is able to rupture the foam films.

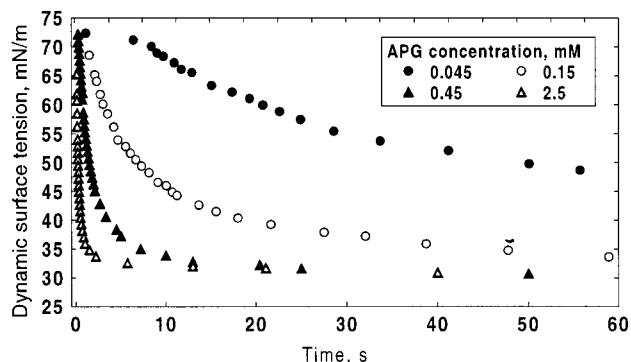
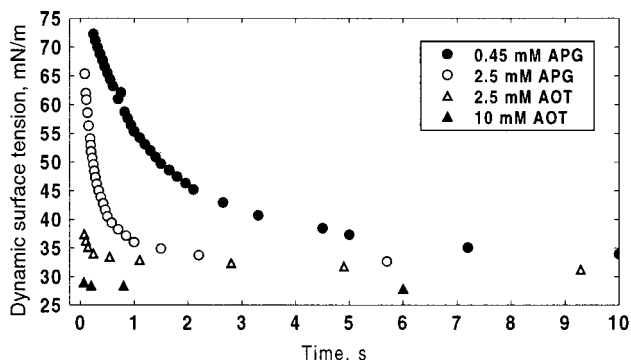
To simulate the conditions during foaming, when the surfaces of the foam films are not saturated with surfactant, we performed FTT experiments with 0.045 mM solutions of APG (about 3 times below cmc). The barrier to globule entry is less than 10 Pa for this system; see Table 3. The latter value is close to the entry barrier of CA and EA globules in 10 mM AOT solutions, where these antifoams are very active. Hence, the entry through incomplete adsorption layers of APG (under dynamic conditions) and the subsequent foam film destruction should be rather easy.

Finally, the addition of 10 mM NaCl into a 0.45 mM APG solution containing EA results in a significant decrease of the entry barrier; almost all of the antifoam globules enter the film surface in the range between 5 and 200 Pa. This is further evidence for the important role of the electrostatic interactions in APG solutions.

**3.5. Dynamic Surface Tension (DST).** The dynamic surface tension,  $\sigma(t)$ , of APG and AOT solutions is measured to obtain information about the kinetics of surfactant adsorption.

The results for  $\sigma(t)$  of APG solutions at four concentrations (0.045, 0.15, 0.45, and 2.5 mM) are shown in Figure 11. At shorter bubbling times, the surface expansion is faster, the surface is depleted of surfactant, and  $\sigma(t)$  is higher. The shortest accessible bubbling time in our equipment ( $\sim 0.1$  s) corresponds to a surface expansion rate of  $<1$  cm<sup>2</sup>/s, which is at least 10 times lower than the rate of surface formation in the foam test used by us. Nevertheless,  $\sigma(t = 0.1)$  is much larger than the equilibrium surface tension at all studied concentrations, which evidences that the solution surface is unsaturated with surfactant during foaming. More than 10 s is necessary for approaching the equilibrium surface tension at 0.45 mM APG. One can conclude that the adsorption of APG molecules is rather slow and the surfaces of the newly formed foam films (in the foam test and in the equipment for vertical films) are very far away from equilibrium.

The results with AOT solutions are rather different. The DST of 10 mM AOT is virtually equal to the

**Figure 11. Dynamic surface tension of APG solutions at different surfactant concentrations (cmc = 0.15 mM).****Figure 12. Dynamic surface tension of AOT and APG solutions; 10 mM AOT and 0.45 mM APG are the concentrations in the foam tests. For comparison, the results for equal surfactant concentration (2.5 mM) are also shown.**

equilibrium one even at the shortest accessible bubbling time (Figure 12). Therefore, the kinetics of surfactant adsorption and the saturation of the bubble surface during foaming are much faster with AOT. This means that the studied antifoams (EA and CA) are able to rupture the foam films even when the film surfaces are covered by equilibrium adsorption layers.

The faster kinetics of adsorption in AOT is primarily due to the higher total concentration of surfactant in the working solutions (10 mM AOT vs 0.45 mM APG). The comparison of the kinetics of adsorption at equal concentrations (2.5 mM) shows, however, that even in this case the AOT adsorption is faster (Figure 12). This result is not trivial, because one may expect that the adsorption of the anionic surfactant should be slower, because of the electrostatic repulsion between the adsorbing molecules and the charged surface.<sup>41–43</sup> The obtained DST data indicate that there are other, more important factors which make the adsorption of APG molecules extremely slow; most probably, the disintegration of the APG micelles is

(41) Dukhin, S. S.; Kretschmar, G.; Miller, R. *Dynamics of Adsorption at Liquid Interfaces*; Elsevier: Amsterdam, 1995.

(42) MacLeod, C.; Radke, C. J. *Langmuir* **1994**, *10*, 3555.

(43) Danov, K. D.; Kolev, V. L.; Kralchevsky, P. A.; Broze, G.; Mehreteab, A. *Langmuir* **2000**, *16*, 2942.

very slow (2.5 mM corresponds to  $17 \times$  cmc for APG, whereas it is just below cmc for AOT).

In conclusion, the mixed antifoams have some reasonable activity in APG solutions mainly because the rate of surfactant adsorption is rather slow; more than 10 s is needed for saturation of the adsorption layer in the working solutions (this process takes less than 0.1 s in AOT solutions). If the kinetics of adsorption of APG was faster at the same height of the entry barrier, the residual foam would be higher and the antifoam would be less efficient.

**3.6. Entry,  $E$ , Spreading,  $S$ , and Bridging,  $B$ , Coefficients.** The values of  $E$ ,  $S$ , and  $B$  can be calculated<sup>2,44</sup> from the interfacial tensions, oil–air,  $\sigma_{OA}$ , solution–air,  $\sigma_{AW}$ , and oil–solution,  $\sigma_{OW}$ :

$$E = \sigma_{AW} + \sigma_{OW} - \sigma_{OA} \quad (4)$$

$$S = \sigma_{AW} - \sigma_{OW} - \sigma_{OA} \quad (5)$$

$$B = \sigma_{AW}^2 + \sigma_{OW}^2 - \sigma_{OA}^2 \quad (6)$$

Two sets of values are considered: initial coefficients (denoted by superscript IN), corresponding to a solution surface free of spread oil, and equilibrium coefficients (superscript EQ), corresponding to a solution surface covered by a spread layer of oil. Positive values of these coefficients are often considered to ensure a high antifoam activity; for analytical discussions of this issue, see refs 2, 24, 25, and 44.

We measured the following values for the interfacial tensions (in mN/m):  $\sigma_{OA} = 20.6$ ,  $\sigma_{OW} = 4.6$ ,  $\sigma_{AW}^{IN} = 28.6$ , and  $\sigma_{AW}^{EQ} = 24.4$ . From these tensions, we calculated  $E^{IN} = 12.6$  mN/m,  $S^{IN} = 3.4$  mN/m, and  $B^{IN} = 415$  (mN/m)<sup>2</sup> and  $E^{EQ} = 8.4$  mN/m,  $S^{EQ} = -0.8$  mN/m (zero in the framework of the experimental accuracy), and  $B^{EQ} = 192$  (mN/m)<sup>2</sup>. Very similar values were previously obtained with AOT solutions,<sup>25</sup> which is direct proof that the differences observed between these two surfactants are not related to the values of  $E$ ,  $S$ , and  $B$ . Moreover, the fact that the studied antifoams are inactive under static conditions at positive  $E$ ,  $S^{IN}$ , and  $B$  emphasizes again the important role of the entry barrier for the antifoam activity.

**3.7. Surface Tension of Exhausted Solutions.** It was found in ref 25 that the direct loading of antifoam emulsions by pipets leads to the transfer of spread oil from the batch emulsion onto the surface of the solutions used in the foam tests. Hence, the surface tension of the working solutions,  $\sigma_{AW}$ , was lowered in comparison with  $\sigma_{AW}^{IN}$ . On the other hand, the surface tension of AOT solutions containing *exhausted* EA was equal to that of pure surfactant solution,  $\sigma_{AW} \approx \sigma_{AW}^{IN}$ , which was a clear indication that the exhaustion is related to emulsification of the spread oil (for more explanations, see ref 26).

To study how the layer of spread oil changes with the antifoam exhaustion in APG solutions, we measured the surface tension in the presence of active and exhausted EA; see Table 4, where the last column shows the difference  $\Delta\sigma = (\sigma_{AW}^{IN} - \sigma_{AW})$ . As expected,  $\sigma_{AW}$  of solutions containing active EA (directly loaded by a pipet) was reduced in comparison with the surface tension of pure APG solution,  $\Delta\sigma = 4.2$  mN/m.

The transfer of oil from the “mother emulsion” onto the surface of the working solutions can be avoided by using the so-called “two-tips procedure” (TTP) described in ref 25. The application of the TTP removes the spread oil

**Table 4. Surface Tension of 0.45 mM APG Solutions in the Absence and in the Presence of EA (Fresh or Exhausted)<sup>a</sup>**

sample	procedure for cell loading	surface tension $\sigma_{AW}$ , mN/m	$\Delta\sigma$ , mN/m
APG		$28.6 \pm 0.2$	
APG with 0.01% fresh emulsion A	directly TTP	$24.4 \pm 0.3$ $28.6 \pm 0.2$	$4.2 \pm 0.5$ $\approx 0$
APG with 0.01% exhausted emulsion A	directly TTP	$30.0 \pm 0.3$ $32.5 \pm 0.7$	$-1.4 \pm 0.5$ $-3.9 \pm 1.0$

<sup>a</sup> The solutions are poured into the experimental container either directly (by a pipet) or by using the two-tips procedure (TTP), which ensures a solution surface free of spread oil (ref 25).

layer, and  $\Delta\sigma$  becomes practically zero for both AOT<sup>25</sup> and APG solutions containing fresh antifoam (see Table 4).

Surprisingly, the surface tension of APG solutions containing exhausted EA was higher in comparison to  $\sigma_{AW}^{IN}$ , that is,  $\Delta\sigma < 0$ . The only explanation we could suggest for this result is that the surfactant concentration in the aqueous phase,  $C_s$ , significantly decreases during exhaustion. One can estimate from the surface tension isotherm of APG that  $C_s$  should be about 0.05 mM (9 times lower than the initial concentration) to obtain  $\Delta\sigma = -3.9$ ; see Table 4. Very similar increase of the surface tension and decrease of the generated foam are obtained when PDMS oil (without silica and Span particles) is dispersed in the APG solution, which shows that the observed effect is not related to the solid particles.

One could hypothesize that the decrease of  $C_s$  is due to surfactant adsorption on the surface of the small oil drops produced during exhaustion. Simple estimates show, however, that this explanation is unrealistic. If we disperse the antifoam into spherical globules of diameter  $d$ , the amount of the adsorbed surfactant is

$$N = S_A/A = 6V_A/(dA) \quad (7)$$

where  $S_A$  is the area of the oil–water interface,  $A$  is the area per molecule in the adsorption layer, and  $V_A$  is the total volume of the antifoam. Taking typical values,  $V_A = 10 \mu\text{L}$ ,  $d = 300$  nm, and  $A = 0.4$  nm<sup>2</sup>, we can estimate that only about  $10^{-6}$  M surfactant can be adsorbed on the antifoam globules. On the other hand, the total amount of surfactant in the foam test is  $4.5 \times 10^{-5}$  M, that is, about 50 times more. Hence, one cannot explain the observed reduction of  $C_s$  by adsorption.

Another possible explanation is that APG (or at least some of the components in this surfactant mixture) has a significant solubility in the silicone oil, so a transfer of surfactant from the aqueous into the oil phase takes place during foaming. Indeed, static and dynamic light scattering experiments with PDMS, that has been pre-equilibrated with APG solution, demonstrate the presence of nanometer sized entities (absent in the original PDMS oil) which are most probably reverse micelles of APG.

The complications with the solubility of APG in PDMS did not allow us to analyze in detail the role of the spread oil in the exhaustion process, as was previously done for AOT.<sup>26</sup> Nevertheless, the fact that the application of TTP to exhausted solutions increases  $\sigma_{AW}$  only by 2.5 mN/m (vs 4.2 mN/m for fresh EA) indicates that probably a molecularly thin oil layer has remained after exhaustion, whereas the surface of the solutions containing fresh EA is covered by a thick oil layer (see section 3.8). Thus, we can conclude that the exhaustion in APG solutions is also related to emulsification of the spread oil as in the AOT solutions.

(44) Aveyard, R.; Binks, B. P.; Fletcher, P. D. I.; Peck, T.-G., Garrett, P. R. *J. Chem. Soc., Faraday Trans.* **1993**, *89*, 4313.

**3.8. Oil Spreading.** Previous experiments<sup>9,26</sup> showed that a thin precursor layer of oil rapidly spreads on the surface of 10 mM AOT solution. Less than 2 s is needed for PDMS to spread up to 5 cm radial distance from the oil source. In equilibrium, a thin PDMS layer ( $\approx 2.6$  nm) coexists on the AOT surface with macroscopic oil lenses.<sup>9</sup>

The experiments with APG solutions showed that the spreading is slower; more than 20 s is needed for radial spreading up to 5 cm. Furthermore, one observes an "induction period"; a PDMS drop deposited on the solution surface first forms a lens which almost does not change its size during 15 s, followed by a rapid expansion of the lens perimeter until a thick oil layer covers the entire solution surface (no precursor film spreading is detected). The observed induction period is another indication for the important role of the slow surfactant adsorption in APG solutions. One can estimate from eq 5 that  $\sigma_{OW}$  should be below 8.0 mN/m for an oil spreading as a thick layer on clean solution surface to take place. However, the interfacial tension of the bare water–PDMS interface is 39 mN/m,<sup>9</sup> which means that a significant adsorption of APG molecules should take place before the spreading may occur.

#### 4. Concluding Remarks

The experiments, aimed to compare the foam destruction process by several mixed solid–liquid antifoams (Table 1) in APG and AOT solutions, showed that the general mechanisms are essentially the same:<sup>25,26</sup>

The foams are destroyed through rupture of the foam films by the bridging–stretching mechanism (Figures 1 and 8).

The main role of the solid particles is to destabilize the asymmetric oil–water–air films, facilitating in this way the entry of the antifoam globules (Figures 9 and 10 and Table 3).

The antifoam exhaustion can be explained by processes of (i) emulsification of the spread oil layer and (ii) partial segregation of the oil and solid particles. The reactivation is due to a recombination of the newly added oil with solid particles from the initially introduced antifoam (Figures 4–6, Table 4, and ref 26).

At the same time, we observed several important differences in the antifoam activity in APG and AOT solutions:

Although the entry, spreading, and bridging coefficients are practically the same for APG and AOT, in general the antifoams are much more active in AOT solutions (sections 3.1 and 3.6).

In APG solutions, the antifoams are active only under dynamic conditions (during foaming); there is a significant residual foam, which is stable for many hours (Table 2).

On the contrary, the antifoams are very active in AOT solutions under both static and dynamic conditions, and the foam is entirely destroyed within seconds even if the system is not agitated.<sup>25</sup>

The antifoams containing solid particles of Span 60 exhibit much higher activity in APG solutions as compared to the antifoams containing only silicone oil and silica. The latter are practically inactive in APG but are very efficient in AOT solutions (section 3.1).

The model experiments show that the above differences can be explained by several simple effects:

The entry barrier is much higher for APG solutions (above 125 Pa) in comparison with AOT (below 20 Pa); see Table 3. Therefore, the antifoam globules are unable to enter the surfaces of the foam films stabilized by APG, if the adsorption surfactant layers are saturated. The entry is possible only if the film surfaces are depleted of surfactant. On the contrary, the globule entry and the subsequent film rupture are possible in AOT solutions even when the adsorption layers are saturated.

The mixed antifoams have some reasonable activity in APG solutions mainly because the rate of surfactant adsorption is rather slow (Figures 11 and 12). If the kinetics of adsorption of APG were faster (at the same height of the entry barrier), the residual foam would be higher and the antifoam would be less efficient.

The high entry barrier in APG solutions is related to the presence of a strong electrostatic repulsion between the surfaces of the asymmetric oil–water–air film and to the small penetration depth of the silica particles into the aqueous phase (Figures 7 and 9). As a result, the silica is unable to break the asymmetric films and to induce a globule entry. The asymmetric films in AOT solutions are much thinner (because of the higher ionic strength); the silica particles protrude deep across the film and break it.

In APG solutions, the penetration depth of the Span particles is much larger than that of silica, and the introduction of Span leads to lower entry barriers (Figure 9 and Table 3).

**Acknowledgment.** This study was supported by Rhodia Silicones Europe (Saint Fons, France). The MBPM measurements were kindly performed by Mrs. I. Surcheva (Sofia University) and the experiments with the high-speed camera were made together with Mr. J.-Y. Martin (Rhodia); their help is gratefully acknowledged. The authors are indebted to Dr. P. Branlard, Dr. Y. Giraud, Dr. P. Cooper, and Dr. M. Deruelle (Rhodia) for many helpful discussions.

LA001558N